Long-term high intake of 9-PAHPA or 9-OAHPA increases basal metabolism and insulin sensitivity but disrupts liver homeostasis in healthy mice

Melha Benlebna, Laurence Balas, Béatrice Bonafos, Laurence Pessemesse, Claire Vigor, Jacques Grober, Florence Bernex, Gilles Fouret, Veronika Paluchova, Sylvie Gaillet, et al.

▶ **To cite this version:**

Melha Benlebna, Laurence Balas, Béatrice Bonafos, Laurence Pessemesse, Claire Vigor, et al.. Long-term high intake of 9-PAHPA or 9-OAHPA increases basal metabolism and insulin sensitivity but disrupts liver homeostasis in healthy mice. Journal of Nutritional Biochemistry, 2020, 79, pp.108361. 10.1016/j.jnutbio.2020.108361 . hal-02532921

HAL Id: hal-02532921

https://institut-agro-dijon.hal.science/hal-02532921

Submitted on 16 Dec 2020

HAL is a multi-disciplinary open access archive for the deposit and dissemination of scientific research documents, whether they are published or not. The documents may come from teaching and research institutions in France or abroad, or from public or private research centers.

L'archive ouverte pluridisciplinaire **HAL**, est destinée au dépôt et à la diffusion de documents scientifiques de niveau recherche, publiés ou non, émanant des établissements d'enseignement et de recherche français ou étrangers, des laboratoires publics ou privés.

Long-term high intake of 9-PAHPA or 9-OAHPA increases basal metabolism and insulin sensitivity but disrupts liver homeostasis in healthy mice

Melha Benlebna[a], Laurence Balas[b], Béatrice Bonafos[a], Laurence Pessemesse[a], Claire Vigor[b], Jacques Grober[c], Florence Bernex[d], Gilles Fouret[a], Veronika Paluchova[f], Sylvie Gaillet[a], Jean François Landrier[e], Ondrej Kuda[f], Thierry Durand[b], Charles Coudray[a], François Casas[a], Christine Feillet-Coudray[a,*]

[a]*DMEM, INRAE, Univ Montpellier, Montpellier, France*
[b]*IBMM, Univ. Montpellier, CNRS, ENSCM, Montpellier, France*
[c]*LNC UMR1231, INSERM, Univ Bourgogne Franche-Comté, Agrosup Dijon, LipSTIC LabEx, Dijon, France*
[d]*INSERM, U1194, Network of Experimental Histology, BioCampus, CNRS, UMS3426, Montpellier, France*
[e]*Aix Marseille Univ, INSERM, INRAE, C2VN, Marseille, France*
[f]*Department of Metabolism of Bioactive Lipids, Institute of Physiology of the Czech Academy of Sciences, Videnska 1083, 142 20 Prague, Czech Republic*

Received 27 September 2019; received in revised form 24 January 2020; accepted 10 February 2020

Abstract

Branched fatty acid esters of hydroxy fatty acids (FAHFAs) are a new family of endogenous lipids recently discovered. Several studies reported that some FAHFAs have antidiabetic and anti-inflammatory effects. The objective of this study was to explore the impact of two FAHFAs, 9-PAHPA or 9-OAHPA, on the metabolism of mice. C57Bl/6J male mice, 6 weeks old, were divided into 3 groups of 10 mice each. One group received a control diet and the two others groups received the control diet supplemented with 9-PAHPA or 9-OAHPA for 12 weeks. Mouse weight and body composition were monitored throughout the study. Some days before euthanasia, energy expenditure, glucose tolerance and insulin sensitivity were also determined. After sacrifice, blood and organs were collected for relevant molecular, biochemical and histological analyses. Although high intake of 9-PAHPA or 9-OAHPA increased basal metabolism, it had no direct effect on body weight. Interestingly, the 9-PAHPA or 9-OAHPA intake increased insulin sensitivity but without modifying glucose tolerance. Nevertheless, 9-PAHPA intake induced a loss of glucose-stimulated insulin secretion. Surprisingly, both studied FAHFAs induced hepatic steatosis and fibrosis in some mice, which were more marked with 9-PAHPA. Finally, a slight remodeling of white adipose tissue was also observed with 9-PAHPA intake. In conclusion, the long-term high intake of 9-PAHPA or 9-OAHPA increased basal metabolism and insulin sensitivity in healthy mice. However, this effect, highly likely beneficial in a diabetic state, was accompanied by manifest liver damage in certain mice that should deserve special attention in both healthy and pathological studies.
© 2020 Elsevier Inc. All rights reserved.

Keywords: FAHFA; Insulin sensitivity; Liver steatosis; Liver fibrosis; Inflammation; Mice

1. Introduction

Recently, a new class of endogenous bioactive lipids, branched fatty acid esters of hydroxy fatty acids (FAHFAs), has been discovered [1]. FAHFAs are a combination of fatty acid (FA) and hydroxylated fatty acid (HFA), and thus, a great diversity of FAHFAs structure exists regarding the numerous types of naturally occurring FA and HFA. Major FAHFAs are a combination of palmitic acid (PA), stearic acid (SA), oleic acid (OA) or palmitoleic acid (PO) with their corresponding HFA providing, for example, PAHPA, OAHPA, PAHOA, OAHOA, PAHSA and OAHSA [2]. It was reported that palmitic acid esters of hydroxystearic acid (PAHSAs) exert antidiabetic and anti-inflammatory effects [1,3], suggesting that it could have a high therapeutic potential to prevent and/or treat type 2 diabetes. However, little if any is known regarding biological effects of other types of FAHFAs. Recently, 9-PAHPA and 9-OAHPA, two FAHFAs shown by Yore et al. [1] to be highly up-regulated in the adipose-specific Glut4 overexpressing *mice* (AG4OX), were synthesized by Balas et al. [4], allowing to study both the biological activities of FAHFAs other than PAHSAs and the influence of FA and HFA chains inside the FAHFA. Regarding human dietary intake of FAHFAs, both PAHPA and OAHPA are present in the diet, in yolk and meat but also in numerous plant foods, with the highest abundancy in strawberry, radish, pineapple, apple and oat [5].

The liver is a key metabolic organ which governs body energy metabolism; it acts as a hub to metabolically connect to various tissues, including skeletal muscle and white adipose tissue (WAT) [6]. In addition, the liver metabolic activity, particularly glucose production, is tightly controlled by insulin [5]. Moreover, mitochondria play a central role in cellular energy metabolism and in metabolic regulation of liver pathophysiology [7]. Indeed, previous work from our team

* Corresponding author at: INRAE UMR 866, 34060 Montpellier, France. Tel.: +33 4 99 61 30 38; fax: +33 4 67 54 56 94.
E-mail address: christine.coudray@inra.fr (C. Feillet-Coudray).

demonstrated that various aspects of mitochondrial activity were modified by changes in diet lipid composition or by bioactive molecules such as polyphenols and ubiquinone [8–11].

Therefore, the aim of this work was to determine whether dietary intake of 9-PAHPA or 9-OAHPA may influence insulin sensitivity and glucose metabolism *in vivo* and to study whether the potential beneficial effects of these FAHFAs are sustained with long-term dietary intake. In addition, the liver being a key metabolic organ tightly controlled by insulin, this study also aimed to determine if 9-PAHPA or 9-OAHPA might affect liver metabolic activity. To address these questions, healthy C57Bl/6J mice were fed a control diet supplemented or not with 9-PAHPA or 9-OAHPA for 12 weeks.

Our results show that the long-term high intake of 9-PAHPA or 9-OAHPA increased basal metabolism and enhanced insulin sensitivity in healthy mice. However, 9-PAHPA or 9-OAHPA intake promoted liver steatosis and fibrosis in some mice, underlining the fact that a likely beneficial effect of these FAHFAs in pathological situations can be harmful in a situation of good health at least at this high dietary intake.

2. Materials and methods

2.1. FAHFAs synthesis

The synthesis of 9-PAHPA and 9-OAHPA was performed using our previously reported procedure [4]. The molecular weight of 9-PAHPA is 510.5 g/mol, and the molecular weight of 9-OAHPA is 537 g/mol.

2.2. Animals and diets

Thirty 6-week-old male C57BL/6J mice (Charles River, L'Arbresle, France), weighing about 22 g, were housed (5 per cage) under conditions of constant temperature (20°C–22°C), humidity (45%–50%) and a standard dark cycle (20:00–08:00 h). The mice were randomized, according to their initial weight, into 3 groups of 10 animals and fed for 12 weeks one of the three following semipurified diets: (1) control diet, (2) control diet+9-PAHPA and (3) control diet+9-OAHPA.

The detailed composition of the control diet is given in the Supplementary Table 1. The control diet contains 5% lipids as a mixture of rapeseed oil, high oleic sunflower oil, sunflower oil and linseed oil (oil mixture of Carrefour). The lipid fraction of the control diet was composed of 12.2% saturated fatty acids, 60.6% monounsaturated fatty acids and 27.3% polyunsaturated fatty acids (Supplementary Table 2). The 9-PAHPA or the 9-OAHPA was incorporated into the diet after dissolution in the oil mixture of Carrefour, and the final content of each FAHFA was set at 300 μmol/kg diet. For a mouse of 25 g that eats 2.5 g diet per day, this corresponds to a FAHFA intake of about 30 μmol/day/kg b.w. of mice (or about 15 mg/day/kg). FAHFAs content was quantified in the three experimental diets (Supplementary Table 3). No 9-PAHPA and 9-OAHPA was found in the control diet. The administered dosage of the studied FAHFAs was based on the work of Yore et al. (2014) [1]. It is also in good agreement with the conditions recently published by Paluchova et al. (2020) [12]. Throughout the study, mice were given free access to food and tap water. Mice body weight was followed weekly, and food consumption was determined every 2 days (week) or 3 days (weekend). Our institution guidelines for the care and use of laboratory animals were observed, and all experimental procedures were approved by the local ethical committee in Montpellier, France (Reference APAFIS#12759-2017121912214385). A detailed scheme of the study design is provided in Fig. 1.

2.3. Body composition analysis

Mice whole-body composition (fat and lean masses) was measured every 2 weeks throughout the study by an EchoMRI-700 whole-body composition analyzer (Echo Medical Systems, Houston, TX, USA) according to the manufacturer's instructions.

2.4. Metabolic analyses

Mice oxygen consumption and carbon dioxide production were measured using a Comprehensive Lab Animal Monitoring System (Columbus Instruments, Columbus, OH, USA). Mice were housed in individual cage inside a controlled cabinet. The environmental enclosure allows precise control over the temperature and light/dark cycle. Male mice were acclimatized individually in metabolic cages with *ad libitum* access to standard control and water for 24 h, prior to a 24-h period of automated recordings. Sample air from individual cages was passed through sensors to determine O_2 and CO_2 content. Sensors were calibrated before each experiment against commercial gas mixtures of accurately determined composition (20.5% O_2, 0.5% CO_2 and 79% N_2). For each mouse, volume of oxygen (VO_2) and volume of carbon dioxide (VCO_2) were measured 111 times in about 24 h. The respiratory exchange ratio (RER) was calculated as the VCO2/VO_2 ratio [13].

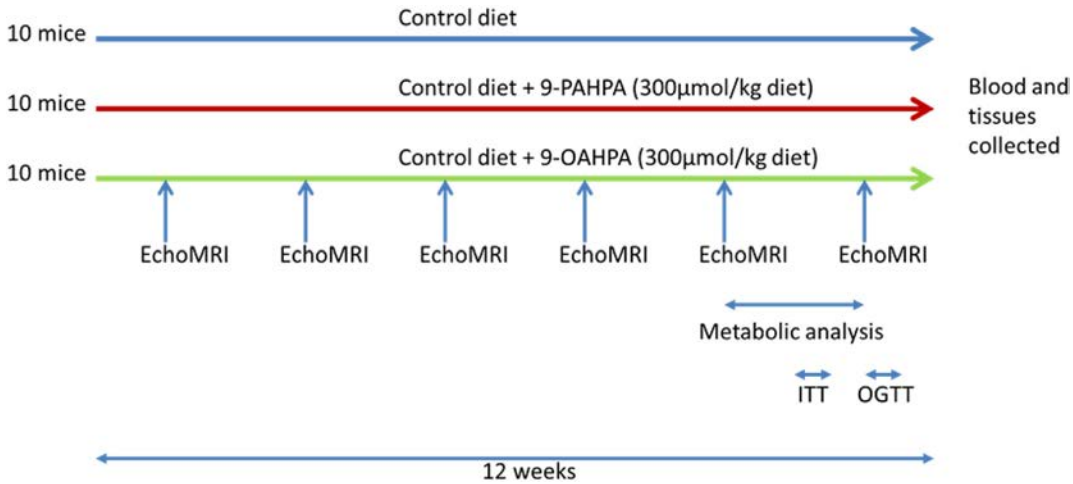

Fig. 1. Design of the study.Thirty 6-week-old male C57BL/6 were fed for 12 weeks a control diet, a control diet+9-PAHPA or a control diet+9-OAHPA. Whole-body composition was measured every 2 weeks using an EchoMRI-700 analyzer. Mice oxygen consumption and carbon dioxide production were measured using a Comprehensive Lab Animal Monitoring System the last weeks of the study. Oral glucose tolerance test and insulin tolerance test were performed the last weeks of the study. At the end of the study, blood was collected from retro-orbital sinus. After cervical dislocation, the liver, WAT and pancreas were removed, rinsed and frozen into liquid nitrogen until analyses.

2.5. Oral glucose tolerance test and insulin tolerance test

Following an overnight fasting, mice were administrated glucose (2 g/kg) by oral gavage, and blood samples were collected from the tail vein at the indicated times for glucose and insulin determination. Insulin tolerance was also assessed after 2-h fasting by administration of human insulin (0.75 U/kg) and blood glucose monitoring. Glycemia was measured using an OneTouch Verio glucometer (Lifescan). Insulin was measured using an ultrasensitive mouse insulin enzyme-linked immunosorbent assay (ELISA) kit (Crystal Chem).

2.6. Sampling and routine biochemical analyses

Four to 5 days after the OGTT or the ITT, blood from 12-h fasted mice was collected from the retro-orbital sinus and distributed into heparinized tubes. Blood tubes were centrifuged at 1000*g* for 10 min at 4°C; plasma was collected and stored at −80°C until analysis. Erythrocytes were washed with saline solution, hemolyzed and stored at −80°C until analysis. After cervical dislocation of mice, liver, WAT and pancreas were removed, rinsed with 0.9% NaCl, weighed and kept at −80°C until analysis.

Plasma levels of glucose, total cholesterol, triglycerides and free fatty acids as well as enzymatic activity of alanine aminotransferase (ALT) were measured at the ANEXPLO/CREFRE analysis platform (CHU RANGUEIL-BP 84225, France). Plasma levels of insulin, leptin and IL-6 were quantified with ELISA kits (Merck Millipore, Darmstadt, Germany; Crystal Chem, Zaandam, Netherlands; Abcam, Paris, France, respectively). Total glucagon-like peptide-1 (GLP-1) plasma concentration was measured by chemiluminescence using commercially available ELISA kit (Mercodia AB, Sweden).

2.7. Liver neutral lipids and histology

To assess liver neutral lipids, liver samples were homogenized in NaCl (9 g/L) and Triton X-100 (0.1%), and free fatty acids, triglycerides and total cholesterol levels were quantified on the tissue homogenate by enzymatic methods (Wako-NEFA-C kit, Oxoid, Dardilly, France; Cholesterol CHOD-PAP SOBIODA kit and triglycerides LQ SOBIODA kit, Sobioda 38330 Montbonnot-Saint-Martin, France) [14].

After euthanasia by cervical dislocation, liver samples were collected, freshly frozen in Tissue-Tek (Microm Microtech) and then stored at −80°C, whereas pancreas were collected, fixed in 4% formaldehyde and then paraffin embedded. For liver, 10-μm sections were stained with Oil Red O or Sirius Red. For Oil Red O staining, the sections were fixed in PBS, 4% PFA at room temperature (RT) 5 min, washed in H_2O, incubated with 60% isopropanol 5 min and then incubated in oil Red O solution (0.6%) 7 min. Then, sections were briefly washed with 60% isopropanol, incubated with Harris' hematoxylin for 30 s, washed in H_2O 3 min and mounted. For Sirius Red staining, the sections were fixed in PBS, 4% PFA at RT 5 min, washed in H_2O and incubated in 0.01% Sirius Red F3B 1 h. Then, sections were washed twice in acidified water, dehydrated thrice in 100% ethanol, then cleared in xylene and mounted. For pancreas, 5-μm sections were stained by hematoxylin and eosin. For the morphometric analysis, liver and pancreatic sections were scanned using a NanoZoomer (Hamamatsu Photonics, Japan) with a 20× objective. The surface of islets was assessed using NDP.View 2 software (Hamamatsu Photonics). The degree of liver fibrosis was evaluated and scored using Image J software as described [15].

2.8. Liver oxidative stress status

2.8.1. Long-established oxidative stress parameters

A part of liver was homogenized in phosphate buffer (50 mM, pH 7) 1 g for 9 ml buffer using a Polytron homogenizer. The liver thiobarbituric acid reactive substances (TBARS) and total glutathione (GSH) levels were measured in homogenate according to the methods of Sunderman [16] and Griffith [17], respectively. The remaining homogenate was centrifuged at 1000*g* for 10 min at 4°C, and the supernatant was used for the other analyses of oxidative stress. Protein oxidation was assessed by measurement of thiol groups [18]. Catalase activity was measured according to the method of Beers and Sizer [19]. Glutathione peroxidase (GPx) was measured according to the method of Flohe and Gunzler [20]. Total superoxide dismutase (SOD) was measured according to the method of Marklund [21].

2.8.2. Isoprostanoid metabolites measurement

To measure oxidative damage to lipids, the liver isoprostanoids levels were measured based on micro-LC–MS/MS technique [22]. Briefly, after lipid extraction with Folch mixture, the extracts were mixed with a cocktail of internal standards, and an alkaline hydrolysis was performed. The metabolites were concentrated thanks to a solid phase extraction step conduced on weak-anion exchange materials. The metabolites were then analyzed by micro-LC–MS/MS. Mass spectrometry analysis was performed in an AB Sciex QTRAP5500 (Sciex Applied Biosystems). The ionization source was electrospray in negative mode. Detection of the fragmentation ion products from each deprotonated molecule was performed in the multiple reaction monitoring modes. Metabolites quantification was done, using MultiQuant 3.0 software, by measuring the ratio of area under the specific metabolite peak/area under the internal standard peak and compared to the ratio of area under the metabolite calibration peak/area under the internal standard peak.

2.9. Liver mitochondrial enzymatic activities

The different mitochondrial respiratory complex activities were determined as previously described [23]. Complex I activity was measured spectrophotometrically at 600 nm during 45 s by following the reduction of 2,6-dichloroindophenol by electrons accepted from decylubiquinol, itself reduced after oxidation of NADH by complex I [24]. Complex II (CII) activity was measured spectrophotometrically at 600 nm by following the reduction of 2,6-dichloroindophenol by the succinate during 120 s [23]. Complex II + III (CII + CIII) activities were measured spectrophotometrically by following the oxidation of oxidation of cytochrome c at 550 nm during 90 s [25]. Cytochrome c oxidase (COX) activity was measured spectrophotometrically by following the oxidation of reduced cytochrome c at 550 nm during 30 s [26]. In addition, mitochondrial β-hydroxyacyl-CoA dehydrogenase (β-HAD), a marker of last step of mitochondrial β-oxidation activity, was determined spectrophotometrically according to the procedure described by Clayton et al. [27].

2.10. Protein isolation and Western blotting analysis

Frozen liver samples were homogenized using an Ultra Turax homogenizer in an ice-cold extraction buffer containing 20 mM Tris–HCL, 150 mM NaCl, 1 mM EDTA, 0.5% Triton X-100, 0.1% SDS, 1 mM PMSF, 10 μM leupeptin and 1 μM pepstatin. Proteins (50 μg) were separated with 6%–15% SDS-PAGE and then transferred to a nitrocellulose membrane (120 min, 100 V). Membranes were blocked in 5% fat-free milk for 1 h at room temperature. Then, membranes were incubated overnight with primary antibody against ChREBP, GLK, GLUT2, IL-6, PEPCK and TNF-α in blocking buffer (Supplementary Table 4). After washes in TBS/Tween under gentle agitation, membranes were incubated for 1 h with horseradish-peroxidase-labeled antibody. After further washes, blots were treated with enhanced chemiluminescence detection reagents (ECL, ThermoScientific, F67403 Illkirch cedex, France). β-Actin or α-tubulin was used as

loading references, and blot intensities were measured using Image Lab Software 5.2.1 (Bio-Rad Laboratories, Inc., France).

2.11. Liver real-time quantitative real-time quantitative polymerase chain reaction (RT-qPCR) analysis

RT-qPCR was used to measure target genes mRNA expression in liver. Total RNA was extracted with Trizol reagent (Invitrogen Life Technologies, Cergy Pontoise, France). Reverse transcription reaction was performed with 2 μg total RNA. cDNA was synthesized with the use of SuperScript II Reverse Transcriptase for first-strand cDNA synthesis (Invitrogen Life Technologies, Cergy Pontoise, France) and Oligo (dT) primers. The mRNA expressions of target genes were determined by RT-qPCR using IQTM SYBR Green Supermix (Biorad, Hercules, CA, USA) with a MiniOpticon detection system (Biorad, Hercules, CA, USA). Results were normalized with the gene encoding RPS9 used as the reference. The primer sequences used for RT-PCR are given in the Supplementary Table 5.

2.12. WAT RT-qPCR analysis

RT-qPCR was applied to measure key inflammation genes mRNA expression in the adipose tissue. RNA from WAT was extracted with Trizol reagent (Invitrogen Life Technologies, Cergy Pontoise, France). Reverse transcription reaction was performed with 1 μg total RNA. cDNA was synthesized with the use of moloney murine leukemia virus reverse transcriptase for first-strand cDNA synthesis and random primers. The mRNA expressions of target genes were determined by RT-qPCR. RT-qPCR analysis was performed using SYBR Green Mastermix (Eurogentec, liege, Belgium) with an Mx3005P Real-Time PCR System (Stratagene, La Jolla, CA, USA). Results were normalized with the gene encoding 18S. The primer sequences used for RT-PCR are given in the Supplementary Table 5.

2.13. WAT lipidomic analysis

2.13.1. Sample extraction

Extraction of WAT metabolites was carried out using a biphasic solvent system of cold methanol, methyl *tert*-butyl ether (MTBE) and water [28] with some modifications. WAT samples (20 mg) were homogenized with 275 μl MeOH and 275 μl 10% MeOH both containing internal standards for 1.5 min using a grinder (MM400, Retsch, Germany). Then, 1 ml of MTBE with internal standard was added, and the tubes were shaken for 1 min and centrifuged at 16,000 rpm for 5 min.

For profiling of high-abundant TAG, 10 μl of upper organic phase was collected, resuspended using a chloroform/MeOH/IPA (1:2:4) mixture, shaken for 30 s and centrifuged at 16,000 rpm for 2 min, and extract was further 100-times diluted with methanol containing CUDA internal standard. For profiling of minor-lipid species in positive and negative ion mode, 100 μl of upper organic phase was collected, resuspended using 80% MeOH with CUDA internal standard, shaken for 30 s, centrifuged at 16,000 rpm for 2 min and used for LC–MS analysis. The LC–MS systems consisted of a Vanquish UHPLC System (Thermo Fisher Scientific, Bremen, Germany) coupled to a QExactive Plus mass spectrometer (Thermo Fisher Scientific, Bremen, Germany).

2.13.2. Lipidomics

Lipids were separated on an Acquity UPLC BEH C18 column (50×2.1 mm; 1.7 μm) coupled to an Acquity UPLC BEH C18 VanGuard precolumn (5×2.1 mm; 1.7 μm) (Waters, Milford, MA, USA). The column was maintained at 65°C at a flow-rate of 0.6 ml/min. For LC–ESI(+)-MS analysis, the mobile phase consisted of (A) 60:40 (v/v) acetonitrile:water with ammonium formate (10 mM) and formic acid (0.1%) and (B) 90:10:0.1 (v/v/v) isopropanol:acetonitrile:water with ammonium formate (10 mM) and formic acid (0.1%). For LC–ESI(−)-MS analysis, the composition of the solvent mixtures was the same with the exception of the addition of ammonium acetate (10 mM) and acetic acid (0.1%) as mobile-phase modifier. Separation was conducted under the following gradient for LC–ESI(+)-MS: 0 min 15% (B); 0–1 min 30% (B); 1–1.3 min from 30% to 48% (B); 1.3–5.5 min from 48% to 82% (B); 5.5–5.8 min from 82% to 99% (B); 5.8–6 min 99% (B); 6–6.1 min from 99% to 15% (B); 6.1–7.5 min 15% (B). For LC–ESI(−)-MS, the following gradient was used: 0 min 15% (B); 0–1 min 30% (B); 1–1.3 min from 30% to 48% (B); 1.3–4.8 min from 48% to 76% (B); 4.8–4.9 min from 76% to 99% (B); 4.9–5.3 min 99% (B); 5.3–5.4 min from 99% to 15% (B); 5.4–6.8 min 15% (B). A sample volume of 0.5–5 μl was used for injection based on extract type. Sample temperature was maintained at 4°C. The source and MS parameters were sheath gas pressure, 60 arbitrary units; aux gas flow, 25 arbitrary units; sweep gas flow, 2 arbitrary units; capillary temperature, 300°C; aux gas heater temperature, 370 °C. For general lipidomics profiling, the mass spectrometer was operated under following conditions: MS1 mass range, *m/z* 200–1700; MS1 resolving power, 35,000 FWHM (*m/z* 200); number of data-dependent scans per cycle, 3; MS/MS resolving power, 17,500 FWHM (*m/z* 200). For ESI(+), spray voltage of 3.6 kV and normalized collision energy of 20% were used, while for ESI(−), spray voltage of −3.0 kV and normalized collision energy of 10%, 20% and 30% were set up. LC–MS and LC–MS/MS data were processed through the software MS-DIAL v. 2.52 [29]. Metabolites were annotated using an in-house retention time–*m/z* library and using MS/MS libraries available from public sources (MassBank, MoNA).

2.14. Statistical analysis

Results were expressed as means±S.D. All the groups were tested for the effects of FAHFAs intake by a one-way analysis of variance (ANOVA) test followed up by a Fisher's least significant difference test. In some case, Student's *t* test was also performed. Correlations were performed with the Kendall method. The limit of statistical significance was set at $P<.05$. The means with different letters were significantly different. Statistical analyses were performed using the StatView program (SAS Institute, Cary, NC, USA).

3. Results

3.1. 9-PAHPA and 9-OAHPA had no effect on food intake, body weight and circulating lipids but increased basal metabolism

Taking into account a mice food intake of about 2.5 g/day, the daily intake of 9-PAHPA or 9-OAHPA correspond to about 0.37 mg FAHFA/day/mouse. The long-term high intake of 9-PAHPA or 9-OAHPA had no effect on body weight, fat and lean mass, food intake and plasma leptin levels (Fig. 2A). Moreover, plasma triglycerides, cholesterol and free fatty acids levels were not affected (Fig. 2B). Serum IL-6 level, a blood marker of inflammation, tended to increase ($P=.0854$) in the 9-PAHPA mice compared to the control and 9-OAHPA mice (Supplementary fig. 1).

In order to investigate the basal metabolism, oxygen consumption and carbon dioxide production were measured using CLAM system. We found that oxygen consumption reflecting the basal metabolism was increased with both 9-PAHPA and 9-OAHPA (respectively, +8% with 9-PAHPA and +17% with 9-OAHPA, $P<.001$) (Fig. 2C). Moreover, analysis of RER revealed that 9-OAHPA but not 9-PAHPA favored the oxidation of carbohydrates, which was reflected by a higher RER value (Fig. 2D).

3.2. 9-PAHPA and 9-OAHPA had no effect on glucose tolerance but improved insulin sensitivity

In both fasting and fed conditions, 9-PAHPA and 9-OAHPA intake had no impact on blood glycemia (Fig. 3A) or on glucose tolerance (Fig. 3B).

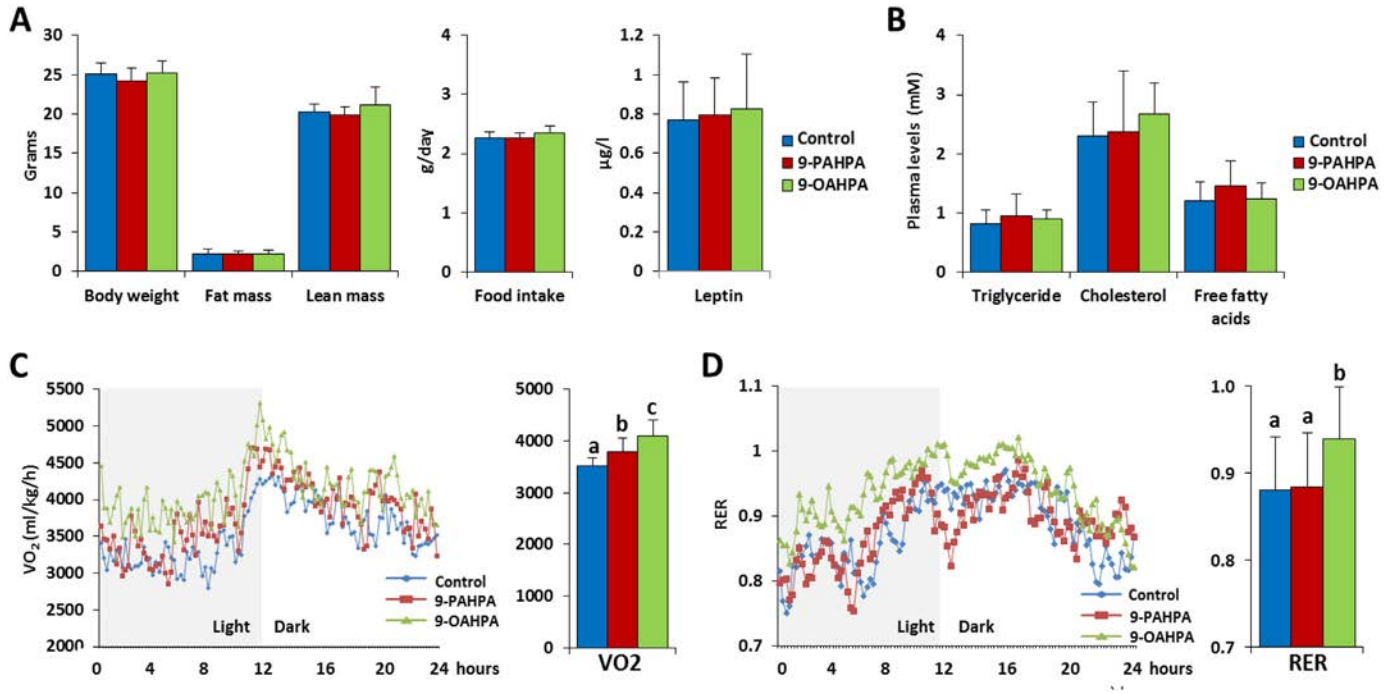

Fig. 2. Mice characteristics.Body weight, fat and lean mass and food intake (A), circulating lipids (B), VO_2 (C) and RER (D) in mice. For each mouse, VO_2 was measured 111 times in about 24 h (Fig. 1A and B). The RER was calculated as the VCO_2/VO_2 ratio (Fig. 1B). Mean VO_2 and RER values are mean of eight mice for each group considering all the cycles (Fig. 1C and D). Results were expressed as means±S.D., $n=111$. All the groups were tested for the effects of FAHFAs intake by a one-way ANOVA test followed up by a Fisher's least significant difference test. The limit of statistical significance was set at $P<.05$. The means with different letters were significantly different.

However, insulin sensitivity was markedly increased by the intake of both 9-PAHPA and 9-OAHPA, and it was even necessary to stop the insulin tolerance test and reinject glucose 30 min after glucose gavage to the 9-PAHPA- or 9-OAHPA-supplemented mice. Indeed, their glycemia levels became so low that these were under the limit of detection of glucometer (Fig. 3C).

The more surprising observation was that plasma insulin levels did not respond to feeding in the 9-PAHPA-supplemented mice, whereas, as expected, they were significantly increased in the control and in 9-OAHPA mice (Fig. 3D). However, insulin levels were significantly higher in 9-PAHPA mice during fasting compared to control and 9-OAHPA mice (ANOVA, $P=.0314$) (Fig. 3D). Fasting level of plasma total GLP-1, an incretin with proven effects in promoting insulin secretion, was not significantly increased in 9-PAHPA or 9-OAHPA mice by comparison to control mice (Fig. 3E). However, plasma total GLP-1 was positively correlated to fasted plasma insulin level ($P=.0394$, $r=0.308$) (Fig. 3F).

3.3. 9-PAHPA or 9-OAHPA intake induced liver alterations in some mice

During mice sacrifice and organs collection, we observed in 3 out of 10 mice fed with 9-PAHPA-supplemented diet and in 1 out of 10 mice fed with 9-OAHPA-supplemented diet a strong alteration of liver appearance (Fig. 4A). However, 9-PAHPA and 9-OAHPA intake had no effect on liver weight compared to control mice (Fig. 4B). In addition, liver content of triglycerides, cholesterol and total lipids was not modified compared to controls, whereas that of free fatty acid was slightly increased only in 9-PAHPA mice (Fig. 4C). Therefore, Oil Red O staining was performed to compare fat accumulation in mice liver. If overall there was no difference among the groups in agreement with previous results of liver lipid content, the livers that were visually strongly altered with 9-PAHPA and 9-OAHPA intake showed an overt accumulation of Oil Red O, suggesting hepatic steatosis in the concerned mice (Fig. 4D). In attempt to explain this high liver lipid content in some mice, we have investigated the gene and/or protein expression of major players in hepatic *de novo* lipogenesis, namely, PPARα, PPARγ, ACC and FAS. Although the obtained results (Supplementary Fig. 2) did not reveal any significant difference among the three studied groups, we however observed a significant correlation between some of these parameters, in particular p-ACC protein abundance, and the hepatic fibrosis index (Supplementary Fig. 3).

Fibrosis was then investigated using Sirius Red staining (Fig. 5A). Fibrosis percentage in liver was increased almost fourfold with 9-PAHPA and about twofold with 9-OAHPA compared to the control mice (Fig. 5B). As observed for Oil Red O staining, the livers that were visually strongly altered with 9-PAHPA and 9-OAHPA intakes presented more important fibrosis. Regarding liver alteration, we showed that plasma ALT activity, a biochemical marker of liver damage, was increased almost threefold with 9-PAHPA and twofold with 9-OAHPA (Fig. 5C). We then studied direct markers of fibrosis using Q-PCR. The expression of MMP2, a metalloproteinase implicated in complex extracellular matrix degradation [30], was significantly increased with 9-PAHPA intake (threefold) but not with 9-OAHPA intake, while gene expression of CoL1A [31], characteristic of liver fibrosis, was nonsignificantly increased (Fig. 5D). As liver fibrosis is often associated to inflammation, we studied specific inflammation markers such as CD68 and MCP-1. However, their expression was not modified by 9-PAHPA or 9-OAHPA intake (Fig. 5E). This result prompted us to study the expression of two major proinflammatory cytokines, TNFα and IL-6, at the protein levels. While liver IL-6 protein expression was unchanged whatever the diet (Fig. 5F), the high intake of both 9-PAHPA and 9-OAHPA significantly decreased liver TNF-α protein expression (Fig. 5G). Interestingly, TNF-α protein expression was inversely correlated to CoL1A ($r=-0.394$, $P=.0048$) (Fig. 5H).

3.4. 9-PAHPA and 9-OAHPA intake had no effect on liver mitochondrial activity and oxidative stress

Because mitochondrial dysfunction and oxidative stress are interconnected and generally known to be involved in the

development of steatohepatitis and fibrosis [32], we investigated these parameters in the mice liver. The enzymatic activities of mitochondrial respiratory chain complexes were not modified by 9-PAHPA and 9-OAHPA, as well as the β-oxidation (Fig. 6A–B). Moreover, the activities of antioxidant enzymes (SOD, MnSOD, catalase and GPx) were not changed either (Fig. 6C). In line with these observations, 9-PAHPA and 9-OAHPA intake had no effect on biochemical markers of oxidized proteins (SH groups and GSSG/GSH) or oxidized lipids (TBARS, phytoprostanes, isoprostanes and neuroprostanes) (Fig. 6D–E).

3.5. High intake of 9-PAHPA slightly altered lipid composition of WAT

Although the fat content of the mice was not changed regardless of the diet (Fig. 2A), the lipidomic analysis of WAT revealed that WAT from 9-PAHPA mice was redesigned and mildly enriched in saturated fatty acids compared to control and 9-OAHPA mice. However, this was observed only in half the mice of this group (Fig. 7A). The WAT mRNA expression of major proinflammatory cytokines (TNFα and IL-6) and chemokines (MCP-1 and RANTES) were not modified whatever the diet (Fig. 7B).

4. Discussion

In the present study, we have investigated for the first time the effect of 9-PAHPA and 9-OAHPA on basal metabolism, insulin sensitivity and glucose tolerance and liver metabolism in control-diet-fed mice. This study is a long-term high intake of 9-PAHPA and 9-OAHPA that lasted 12 weeks. The administered dosage of our FAHFAs was based on the work of Yore et al. (2014) [1]. It is also in good agreement with the conditions recently published by Paluchova et al. (2019) [12]. We have to outline that these high dosages of FAHFAs applied in the present work cannot be taken up through normal dietary. We studied such high dosages in healthy mice because these

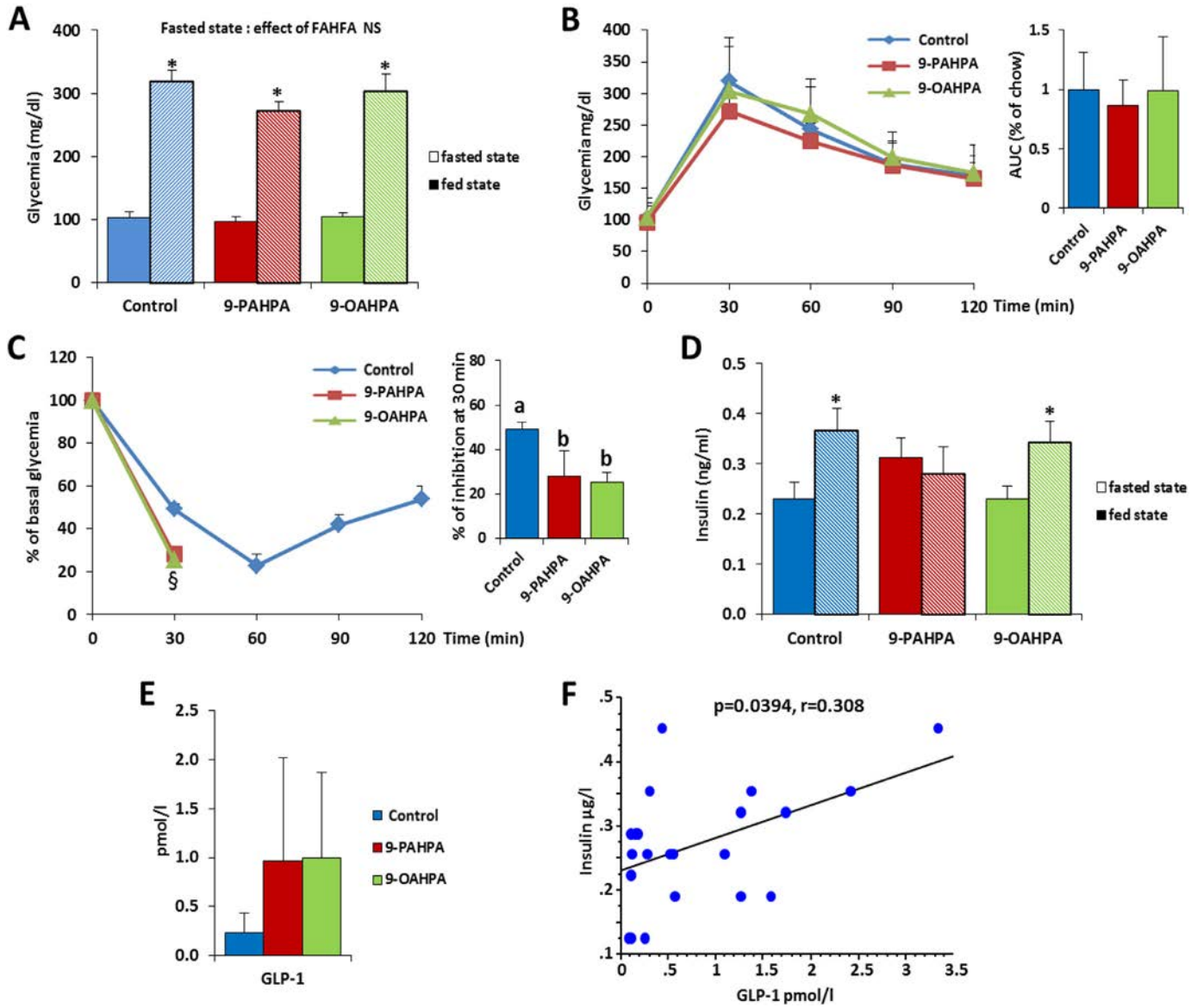

Fig. 3. Glucose and insulin parameters.Glycemia in fast and fed state (A), OGTT (B), ITT (C), plasma insulin (D) level in fast and fed state, plasma total GLP-1 level (E) and correlation between plasma total GLP-1 and circulating insulin (F). Results were expressed as means±S.D., n=8–10 animals per group. Student's t test for comparison between fasted or fed state (30-min glucose injection) inside the same diet. The limit of statistical significance was set at *P<.05 inside of fasted and fed states separately among control and FAHFAs. ANOVA between groups inside fasted state or fed state (30-min glucose injection). For plasma total GLP-1, all the groups were tested for the effects of FAHFAs intake by a one-way ANOVA test followed up by a Fisher's least significant difference test. The limit of statistical significance was set at P<.05. The means with different letters were significantly different.

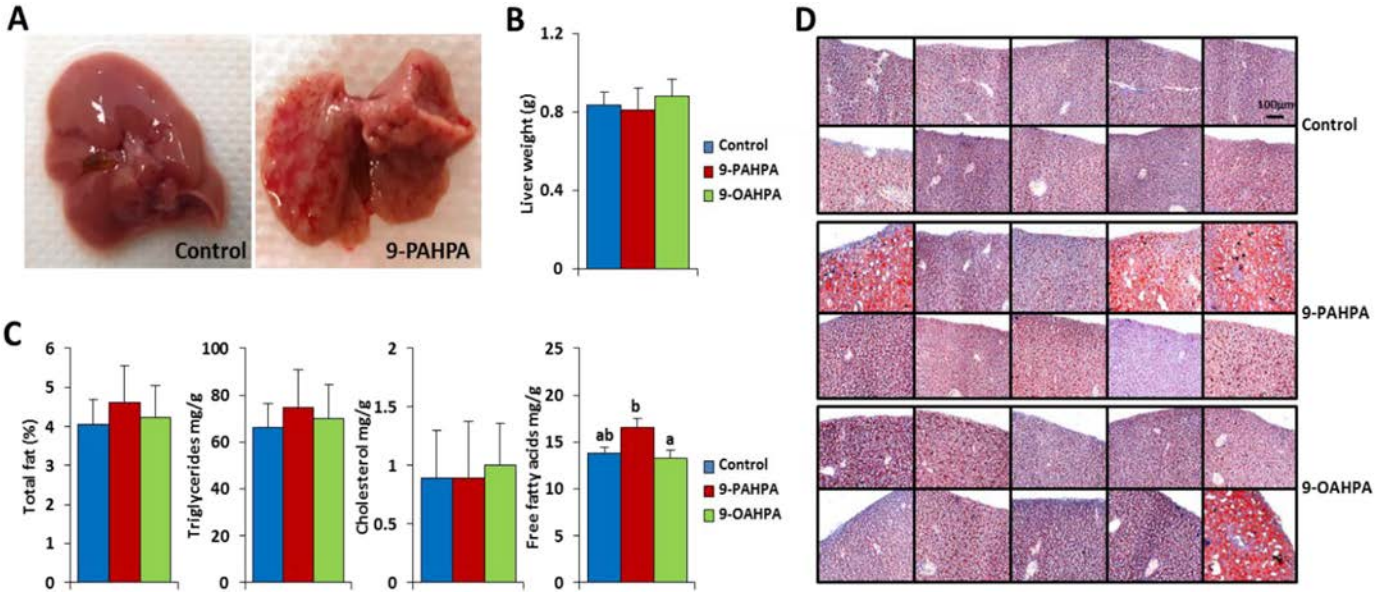

Fig. 4. Liver morphology and steatosis.Visual observation of liver after euthanasia of mice (A), liver weight after 12 weeks of diet (B), hepatic lipid content measured on tissue homogenate by enzymatic methods (C). Results were expressed as means±S.D., n=9–10 animals per group. All the groups were tested for the effects of FAHFAs intake by a one-way ANOVA test followed up by a Fisher's least significant difference test. The limit of statistical significance was set at P<.05. The means with different letters were significantly different. Representative Oil Red O (D) of livers from all the mice (magnification ×10), n=10 animals per group.

dosages were investigated in different pathological situations; therefore, it seemed relevant to study their effects at these dosages in healthy mice as well [1,2,12,33].

4.1. 9-PAHPA and 9-OAHPA increased basal metabolic rate in healthy mice

Our data show for the first time that basal metabolic rate, measured by the rate of oxygen consumption, was increased with both 9-PAHPA and 9-OAHPA intakes but without impact on body weight. No comparison can be made with other types of FAHFAs, as this parameter has never been previously measured following the intake of other FAHFAs.

Our results also show that food intake and adiposity were not altered by 12-week intake of 9-PAHPA or 9-OAHPA. In fact, their dietary intake had no effect on food consumption, body weight or fat mass of mice. This is rather a surprising result because given the effect of 9-PAHPA and 9-OAHPA on basal metabolism, we would have expected a reduction in the weight of mice that eat less. This may suggest that 9-PAHPA and 9-OAHPA could modulate nutrient intestinal absorption. In addition, plasma leptin levels, an anorexigenic hormone mediator of long-term regulation of energy balance [34], was not modified whatever the diet. Circulating lipid levels also remained unchanged. In accordance, Syed et al. [35] observed no effect on all these parameters in mice gavaged for 18 weeks with two structurally different FAHFAs: the 5-PAHSA and 9-PAHSA. These observations show that 9-PAHPA, 9-OAHPA, 5-PAHSA and 9-PAHSA have no effect on food consumption and body fat mass accumulation in control-diet-fed mice. Regarding the numerous different types of FAHFAs that may exist, depending of the FA and HFA structure and the esterification position, this cannot be extrapolated to all FAHFAs and needs to be investigated for each individual FAHFA.

4.2. 9-PAHPA and 9-OAHPA increased insulin sensitivity in healthy mice

The glucose and insulin tolerance tests are useful tools to investigate glucose metabolism. Our study demonstrates that long-term high intake of 9-PAHPA or 9-OAHPA markedly increased insulin sensitivity. In accordance with this observation, experiments performed using metabolic cages showed that, compared to control animals, mice supplemented with 9-OAHPA used glucose preferentially, as evidenced by the increase in the RER. In addition, the lack of increased RER in animals supplemented with 9-PAHPA could probably be explained by the fact that these mice no longer secrete insulin in response to glucose. However, since we did not find any alterations in the morphology and density of the islets of Langerhans in pancreas suggesting an attack of this tissue (Supplementary Fig. 4), we hypothesize that this loss of insulin secretion in response to glucose is probably an adaptation at the β-cell level that has been implemented in these mice to counteract the negative effects of insulin in the liver due to their hypersensitivity to the hormone.

Despite increased insulin sensitivity in 9-PAHPA and 9-OAHPA mice, glucose tolerance was not changed by any diet probably because glucose tolerance is already satisfactory in healthy mice. Regarding molecular glucose metabolism in the liver, the protein expression of Glut-2 (involved in glucose transport), GLK (a major component of the hepatic glucose-sensing system), PEPCK (a key molecule of gluconeogenesis) and ChREBP (a key player in the induction of genes of *de novo* fatty acid synthesis in response to glucose) remained unchanged after 9-PAHPA or 9-OAHPA intake (Supplementary Fig. 5), which indicates that glucose metabolism itself was not affected by the intake of these FAHFAs.

4.3. 9-PAHPA and 9-OAHPA intake induced liver steatosis and fibrosis in some healthy mice

Visual observation of liver after euthanasia of mice revealed severe alterations of some livers in the groups supplemented with 9-PAHPA or 9-OAHPA. Histological analysis revealed steatosis and fibrosis in these same livers. Increased hepatic *de novo* lipogenesis is a significant pathway contributing to nonalcoholic fatty liver disease [36], and it is likely that both FAHFAs have insulin-sensitized the liver of some mice so much that *de novo* lipogenesis promoted steatosis/fibrosis. Although the gene/protein expression analysis of some major players in hepatic *de novo* lipogenesis, namely, PPARα, PPARγ, ACC and FAS, did not reveal significant differences among the three studied groups, it is not excluded that posttranslation protein modifications may be

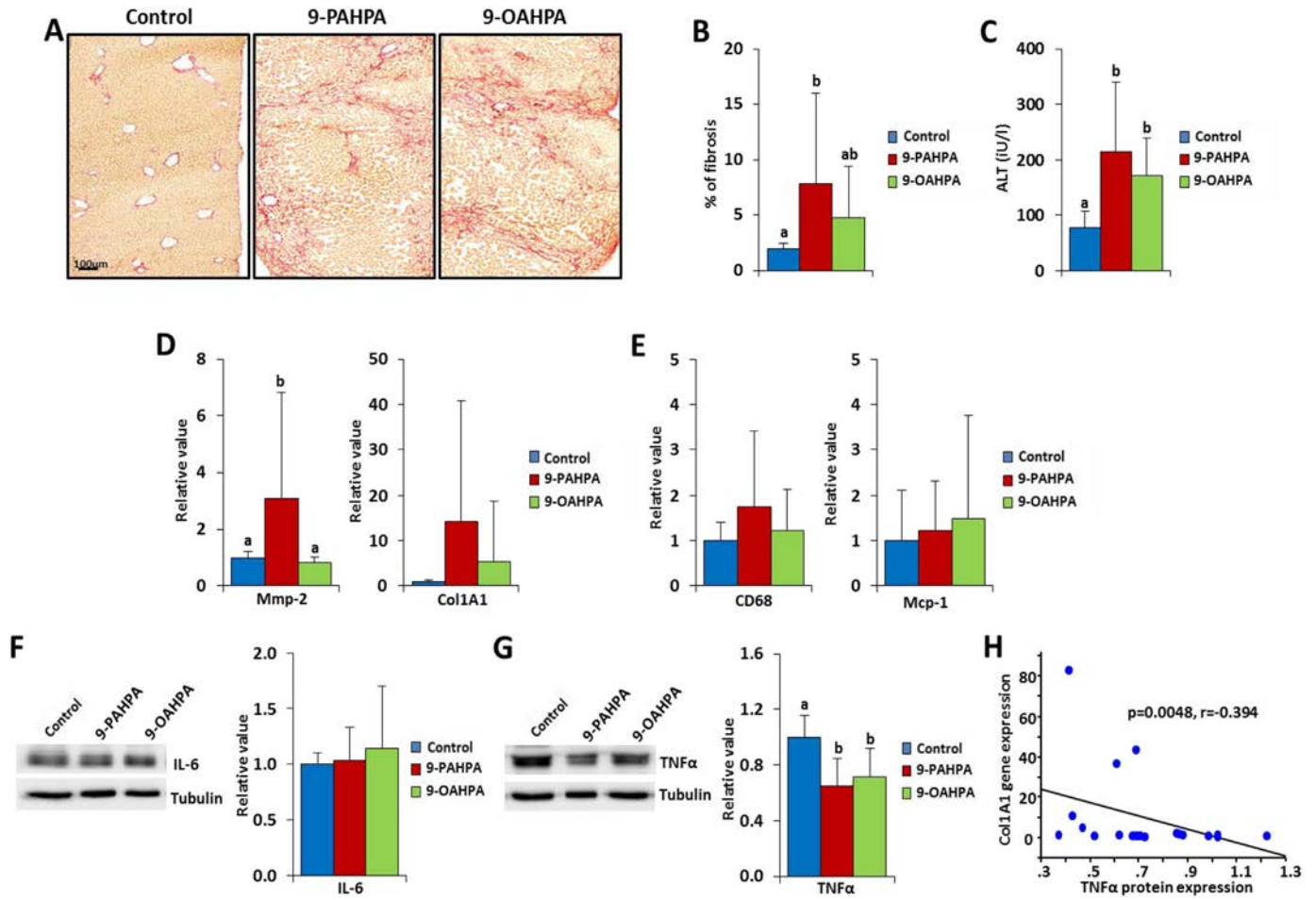

Fig. 5. Liver fibrosis.Sirius Red stains of livers. Pictures are representative from each group (magnification ×10) (A), % of fibrosis (B) and plasma ALT level (C). Gene expression of liver fibrosis markers (D) and liver inflammation markers (E) by qPCR. Protein expression of IL-6 (F) and TNF-α (G) by Western blot and representative pictures from each group. (H) Correlation between TNF-α protein expression and Col1A1 gene expression. Results were expressed as means±S.D., n=9–10 animals per group. All the groups were tested for the effects of FAHFAs intake by a one-way ANOVA test followed up by a Fisher's least significant difference test. The limit of statistical significance was set at P<.05. The means with different letters were significantly different. ALT, alanine aminotransferase; MMP2, matrix metalloproteinase-2; Col1A, collagen type α1; CD68, cluster of differentiation 68; Mcp1, monocyte chemoattractant protein 1; TNFα, tumor necrosis factor α; IL-6, interleukin 6.

involved in the alteration of *de novo* lipogenesis. Nevertheless, histological observations were supported by the gene expression analysis of some liver fibrosis markers linked to matrix degradation [37]. Plasma ALT levels, a biochemical marker of liver damage, confirmed also liver alterations with 9-PAHPA and 9-OAHPA as ALT levels were increased almost threefold with 9-PAHPA and twofold with 9-OAHPA.

In attempt to understand the origin of the liver fibrosis observed in some mice fed with the FAHFA-supplemented diet, we then explored various markers of inflammation. However, neither protein expression of IL-6 nor gene expression of IL-6, TNF-α, MCP-1 and CD-68 was increased whatever the diet. Even more surprisingly, protein expression of TNF-α was significantly decreased in mice liver fed the 9-PAHPA or 9-OAHPA and was inversely correlated to gene expression of one liver fibrosis marker. TNF-α is a multifunctional cytokine that plays important roles in diverse cellular events such as cell survival, proliferation, differentiation and cell death [38], and anti-TNF-α may exert some undesirable effects on liver [39–41].

Liver free fatty acid accumulation, inflammation, oxidative stress and mitochondrial dysfunction generally lead to steatosis and progressively switch it to steatohepatitis [32]. However, free fatty acids rather than triglycerides are responsible for liver injury *via* increased oxidative stress [42]. To explore whether the accumulation of free fatty acids induced oxidative stress, various markers of oxidative stress were investigated as oxidized lipids (isoprostanoids and TBARs), oxidized protein (thiols and glutathione) and antioxidant enzyme activity. Surprisingly, none of these parameters was significantly modified regardless of the diet. Mitochondria are known to be one of the main ROS generation sites within the cell, and mitochondrial ROS production is closely associated with the respiratory chain complexes activity [23]. Moreover, mitochondria are postulated to play a central role in the progression of liver diseases [43]. However, the enzymatic activity of mitochondrial respiratory chain complexes was not modified whatever the diet.

4.4. 9-PAHPA and 9-OAHPA had slight effect on WAT

The WAT lipidomic analysis revealed that 9-PAHPA intake induced a mild enrichment in saturated fats in the WAT of some mice. The mild enrichment in saturated fats of the WAT may be resulting either from the absorption of palmitate as a nutrient fatty acid or from the higher bioavailability of PAHPA. While hepatic *de novo* lipogenesis is thought to contribute to metabolic disease [44], WAT *de novo* lipogenesis is good, promoting "healthy" adipocyte [45]. In accordance, there was no increase of proinflammatory markers in this tissue.

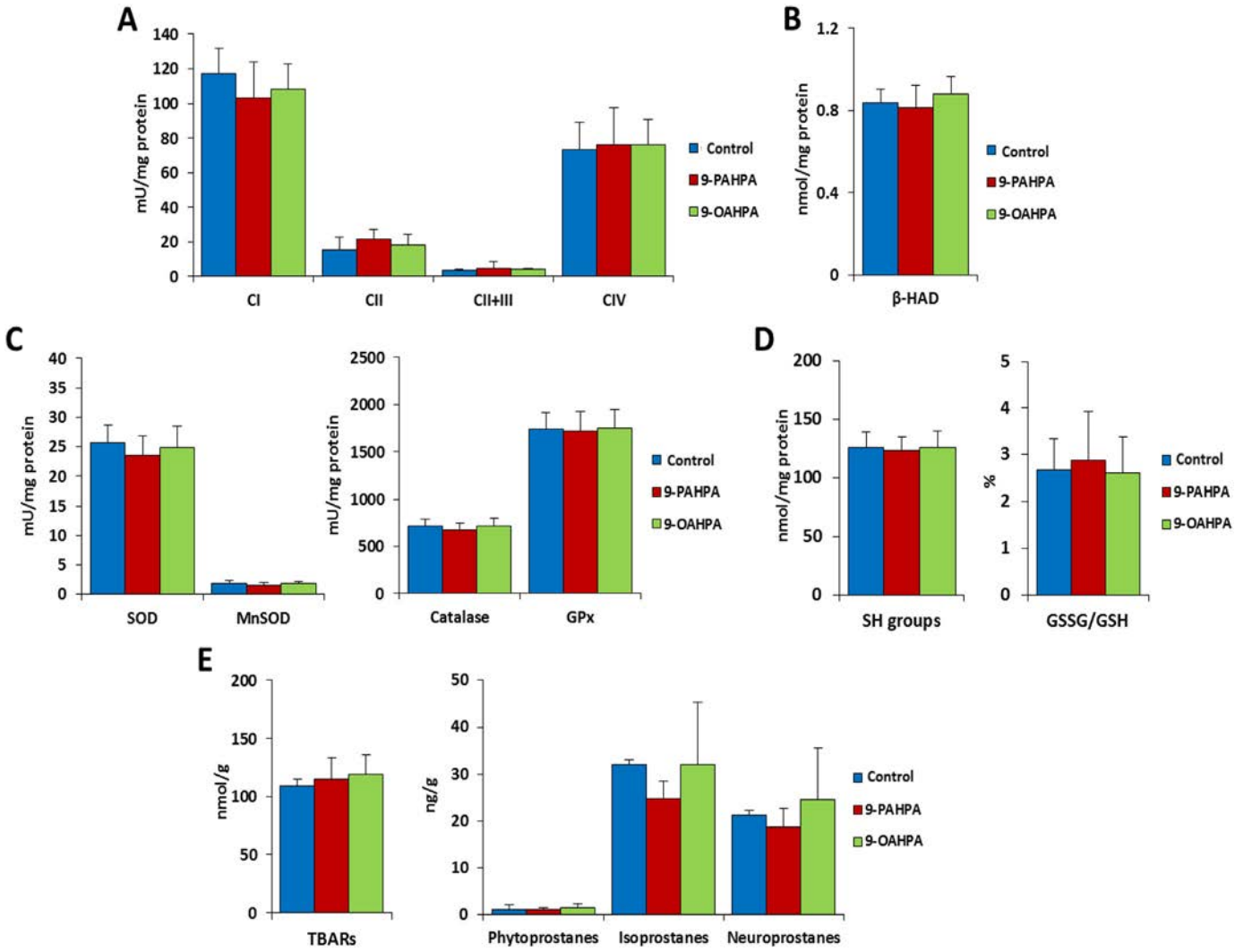

Fig. 6. Mitochondrial activity and hepatic oxidative stress parameters.Results were expressed as means±S.D., n=9–10 animals per group. All the groups were tested for the effects of FAHFAs intake by a one-way ANOVA test followed up by a Fisher's least significant difference test. The limit of statistical significance was set at P<.05. The means with different letters were significantly different. CI, complex I; CII, complex II; CII + III, complexes II + III; COX, cytochrome c oxidase; β-HAD, β-hydroxyacyl-CoA dehydrogenase; SOD, total superoxide dismutase; MnSOD, manganese superoxide dismutase; GPx, glutathione peroxidase; -SH, thiols; GSSG/GSH, oxidized glutathione/reduced glutathione; TBARS, thiobarbituric acid reactive substances. Phytoprostanes: ent-16B1t-phytoprostane, ent-9L1t-phytoprostane, ent-16(RS)-13-epi-ST-d14-9-phytofuran; isoprostanes: 15(S)-F2t-isoprostane, 15(R)-F2t-isoprostane, 5(RS)-5-F2t-isoprostane, 5(RS)-5-F2c-isoprostane; neuroprostanes: 10(S)-F4t-neuroprostane, 10(R)-F4t-neuroprostane, 4(RS)-4-F4t-neuroprostane.

5. Conclusion

This work demonstrates that long-term high intake of 9-PAHPA or 9-OAHPA, incorporated into a control diet, has some positive effects in healthy mice, namely, an increase in basal metabolic rate and in insulin sensitivity. However, 9-PAHPA intake and to a lesser extent 9-OAHPA intake induced liver steatosis and fibrosis in some mice. It is likely that both FAHFAs have insulin-sensitized the healthy liver so much that *de novo* lipogenesis promoted steatosis/fibrosis. This work highlights the fact that long-term high intake of some FAHFAs, because of their high insulin-sensitizing effect, can induce unexpected adverse metabolic effects in healthy mice. The results obtained in the present study are encouraging concerning the effects of these FAHFAs in pathological situations as diabetes. It should be emphasized that the studied FAHFAs cannot be taken up in the concentrations used in this study through normal diet. *In vivo* dose–response studies should be considered to determine the safe intake of 9-PAHPA and 9-OAHPA.

Authors' declaration

Author contributions were as follows: study design (C.C., F.C., C.F.-C.), FAHFAs synthesis (L.B., M.B.), data collection (M.B., B.B., L.P., J.G., G. F., V.P., C.V., S.G., J.F.L., O.K.), statistical analysis (C.C., M.B., F.C., C.F.-C.), data interpretation (M.B., C.C., F.C., F.B., S.G., O.K., T.D., L.B., C.F.-C.), manuscript preparation (M.B., C.C., O.K., L.B., F.C., C.F.-C.), literature search (M.B., C.C., F.C., C.F.-C.) and funds collection (C.C., O.K., F.C., C.F.-C.). All the authors have read and approved the final version of this manuscript.

Acknowledgments

The authors wish also to thank the animal staff from Metamus DMEM facility which belongs to Montpellier animal facilities network (RAM, Biocampus), Biocampus for technical support and expertise for metabolism phenotyping, and Metamontp platform supported by the

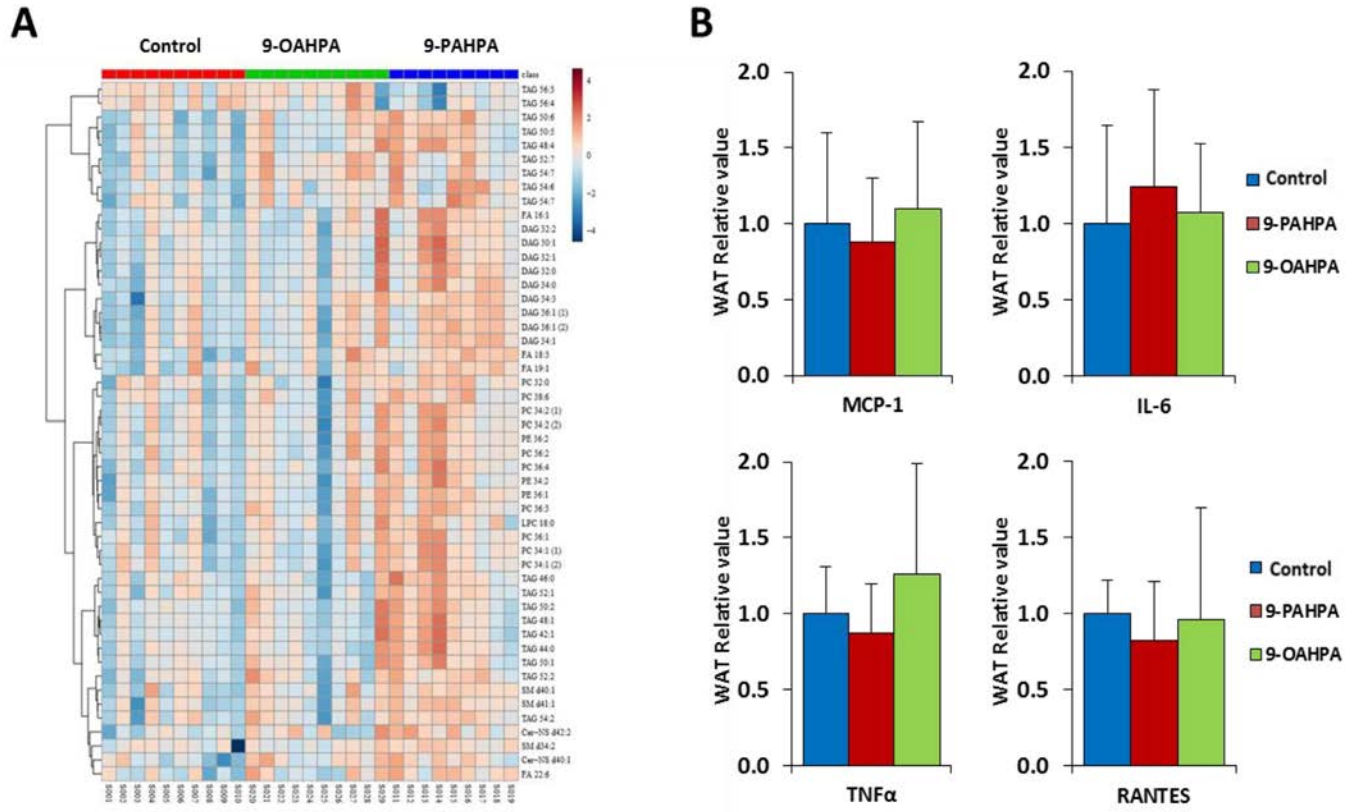

Fig. 7. WAT lipidomic and inflammation.Lipidomic analysis of WAT (A) according to Cajka et al. [28]. Gene expression of WAT inflammation markers (B) by qPCR. Results were expressed as means±S.D., $n=9–10$ animals per group. All the groups were tested for the effects of FAHFAs intake by a one-way ANOVA test followed up by a Fisher's least significant difference test. The limit of statistical significance was set at $P<.05$. The means with different letters were significantly different. Mcp1, monocyte chemoattractant protein 1; IL-6, interleukin 6; TNFα, tumor necrosis factor α; RANTES, regulated upon activation, normal T cell expressed, and secreted.

European fund for the regional development of Occitanie (FEDER). The authors wish to express their deep acknowledgements to Guillaume Reversat, Amandine Rocher and Camille Oger for their technical aid in the isoprostanoid analysis, Annabelle Tavernier for her technical aid in the GLP-1 analysis and Tomas Cajka (Institute of Physiology CAS) for the lipidomic analysis.

Conflict of interest

The authors confirm that this article content has no conflict of interest.

Funding

Melha Benlebna acknowledges the financial support from Ph.D. program of the Algerian Ministry of Higher Education and Scientific Research. The authors acknowledge the financial support of the French Lipid Nutrition Group, the National Institute for Agronomic Research, in particular the Human Nutrition Department (Alim-H department) and Czech Science Foundation (17-10088Y).

Appendix A. Supplementary data

Supplementary data to this article can be found online at

.

References

[1] Yore MM, Syed I, Moraes-Vieira PM, Zhang T, Herman MA, Homan EA, et al. Discovery of a class of endogenous mammalian lipids with anti-diabetic and anti-inflammatory effects. Cell 2014;159:318–32.

[2] Balas L, Feillet-Coudray C, Durand T. Branched fatty acyl esters of hydroxyl fatty acids (FAHFAs), appealing beneficial endogenous fat against obesity and type-2 diabetes. Chemistry 2018;24:9463–76.

[3] Moraes-Vieira PM, Saghatelian A, Kahn BB. GLUT4 expression in adipocytes regulates *de novo* lipogenesis and levels of a novel class of lipids with antidiabetic and anti-inflammatory effects. Diabetes 2016;65:1808–15.

[4] Balas L, Bertrand-Michel J, Viars F, Faugere J, Lefort C, Caspar-Bauguil S, et al. Regiocontrolled syntheses of FAHFAs and LC-MS/MS differentiation of regioisomers. Org Biomol Chem 2016;14:9012–20.

[5] Liberati-Cizmek AM, Bilus M, Brkic AL, Baric IC, Bakula M, Hozic A, et al. Analysis of fatty acid esters of hydroxyl fatty acid in selected plant food. Plant Foods Hum Nutr 2019;74:235–40.

[6] Rui L. Energy metabolism in the liver. Compr Physiol 2014;4:177–97.

[7] Sato N. Central role of mitochondria in metabolic regulation of liver pathophysiology. J Gastroenterol Hepatol 2007;22(Suppl. 1):S1–6.

[8] Aoun M, Feillet-Coudray C, Fouret G, Chabi B, Crouzier D, Ferreri C, et al. Rat liver mitochondrial membrane characteristics and mitochondrial functions are more profoundly altered by dietary lipid quantity than by dietary lipid quality: effect of different nutritional lipid patterns. Br J Nutr 2012;107:647–59.

[9] Fouret G, Tolika E, Lecomte J, Bonafos B, Aoun M, Murphy MP, et al. The mitochondrial-targeted antioxidant, MitoQ, increases liver mitochondrial cardiolipin content in obesogenic diet-fed rats. Biochim Biophys Acta 1847;2015:1025–35.

[10] Hokayem M, Blond E, Vidal H, Lambert K, Meugnier E, Feillet-Coudray C, et al. Grape polyphenols prevent fructose-induced oxidative stress and insulin resistance in first-degree relatives of type 2 diabetic patients. Diabetes Care 2013;36:1454–61.

[11] Feillet-Coudray C, Fouret G, Casas F, Coudray C. Impact of high dietary lipid intake and related metabolic disorders on the abundance and acyl composition of the unique mitochondrial phospholipid, cardiolipin. J Bioenerg Biomembr 2014;46:447–57.

[12] Paluchova V, Oseeva M, Brezinova M, Cajka T, Bardova K, Adamcova K, et al. Lipokine 5-PAHSA is regulated by adipose triglyceride lipase and primes adipocytes for *de novo* lipogenesis in mice. Diabetes 2020;69(3):300–12.

[13] Marvyn PM, Bradley RM, Mardian EB, Marks KA, Duncan RE. Data on oxygen consumption rate, respiratory exchange ratio, and movement in C57BL/6J female mice on the third day of consuming a high-fat diet. Data Brief 2016;7:472–5.

[14] Coudray C, Fouret G, Lambert K, Ferreri C, Rieusset J, Blachnio-Zabielska A, et al. A mitochondrial-targeted ubiquinone modulates muscle lipid profile and improves mitochondrial respiration in obesogenic diet-fed rats. Br J Nutr 2016;115:1155–66.

[15] Standish RA, Cholongitas E, Dhillon A, Burroughs AK, Dhillon AP. An appraisal of the histopathological assessment of liver fibrosis. Gut 2006;55:569–78.

[16] Sunderman Jr FW, Marzouk A, Hopfer SM, Zaharia O, Reid MC. Increased lipid peroxidation in tissues of nickel chloride-treated rats. Ann Clin Lab Sci 1985;15:229–36.
[17] Griffith OW. Determination of glutathione and glutathione disulfide using glutathione reductase and 2-vinylpyridine. Anal Biochem 1980;106:207–12.
[18] Faure P, Lafond J. Measurement of plasma sulfhydryl and carbonyl groups as a possible indicator of protein oxidation. In: Favier A, Cadet J, Kalyanaraman B, Fontecave M, Pierre J, editors. Analysis of free radicals in biological systems. Basel (Switzerland): Birkhauser Verlag 1995. p. 237–48.
[19] Beers Jr RF, Sizer IW. A spectrophotometric method for measuring the breakdown of hydrogen peroxide by catalase. J Biol Chem 1952;195:133–40.
[20] Flohe L, Gunzler WA. Assays of glutathione peroxidase. Methods Enzymol 1984; 105:114–21.
[21] Marklund S. Spectrophotometric study of spontaneous disproportionation of superoxide anion radical and sensitive direct assay for superoxide dismutase. J Biol Chem 1976;251:7504–7.
[22] Dupuy A, Le Faouder P, Vigor C, Oger C, Galano JM, Dray C, et al. Simultaneous quantitative profiling of 20 isoprostanoids from omega-3 and omega-6 polyunsaturated fatty acids by LC-MS/MS in various biological samples. Anal Chim Acta 2016;921:46–58.
[23] Feillet-Coudray C, Sutra T, Fouret G, Ramos J, Wrutniak-Cabello C, Cabello G, et al. Oxidative stress in rats fed a high-fat high-sucrose diet and preventive effect of polyphenols: involvement of mitochondrial and NAD(P)H oxidase systems. Free Radic Biol Med 2009;46:624–32.
[24] Janssen AJ, Trijbels FJ, Sengers RC, Smeitink JA, van den Heuvel LP, Wintjes LT, et al. Spectrophotometric assay for complex I of the respiratory chain in tissue samples and cultured fibroblasts. Clin Chem 2007;53:729–34.
[25] Rustin P, Chretien D, Bourgeron T, Gerard B, Rotig A, Saudubray JM, et al. Biochemical and molecular investigations in respiratory chain deficiencies. Clin Chim Acta 1994;228:35–51.
[26] Wharton D, Tzagoloff A. Cytochrome oxidase from beef heart mitochondria. Methods Enzymol 1967;10:245–50.
[27] Clayton PT, Eaton S, Aynsley-Green A, Edginton M, Hussain K, Krywawych S, et al. Hyperinsulinism in short-chain L-3-hydroxyacyl-CoA dehydrogenase deficiency reveals the importance of beta-oxidation in insulin secretion. J Clin Invest 2001; 108:457–65.
[28] Cajka T, Smilowitz JT, Fiehn O. Validating quantitative untargeted lipidomics across nine liquid chromatography–high-resolution mass spectrometry platforms. Anal Chem 2017;89:12360–8.
[29] Tsugawa H, Cajka T, Kind T, Ma Y, Higgins B, Ikeda K, et al. MS-DIAL: data-independent MS/MS deconvolution for comprehensive metabolome analysis. Nat Methods 2015;12:523–6.
[30] Duarte S, Baber J, Fujii T, Coito AJ. Matrix metalloproteinases in liver injury, repair and fibrosis. Matrix Biol. 2015;44–46:147–56.
[31] Hayashi M, Nomoto S, Hishida M, Inokawa Y, Kanda M, Okamura Y, et al. Identification of the collagen type 1 alpha 1 gene (COL1A1) as a candidate survival-related factor associated with hepatocellular carcinoma. BMC Cancer 2014;14:108.
[32] Manne V, Handa P, Kowdley KV. Pathophysiology of nonalcoholic fatty liver disease/nonalcoholic steatohepatitis. Clin Liver Dis 2018;22:23–37.
[33] Smith U, Kahn BB. Adipose tissue regulates insulin sensitivity: role of adipogenesis, de novo lipogenesis and novel lipids. J Intern Med 2016;280: 465–75.
[34] Klok MD, Jakobsdottir S, Drent ML. The role of leptin and ghrelin in the regulation of food intake and body weight in humans: a review. Obes Rev 2007;8:21–34.
[35] Syed I, Lee J, Moraes-Vieira PM, Donaldson CJ, Sontheimer A, Aryal P, et al. Palmitic acid hydroxystearic acids activate GPR40, which is involved in their beneficial effects on glucose homeostasis. Cell Metab 2018;27:419–27.
[36] Chiu S, Mulligan K, Schwarz JM. Dietary carbohydrates and fatty liver disease: de novo lipogenesis. Curr Opin Clin Nutr Metab Care 2018;21:277–82.
[37] Mak KM, Mei R. Basement membrane type IV collagen and laminin: an overview of their biology and value as fibrosis biomarkers of liver disease. Anat Rec (Hoboken) 2017;300:1371–90.
[38] Wang X, Lin Y. Tumor necrosis factor and cancer, buddies or foes? Acta Pharmacol Sin 2008;29:1275–88.
[39] French JB, Bonacini M, Ghabril M, Foureau D, Bonkovsky HL. Hepatotoxicity associated with the use of anti-TNF-alpha agents. Drug Saf 2016;39:199–208.
[40] Ghabril M, Bonkovsky HL, Kum C, Davern T, Hayashi PH, Kleiner DE, et al. Liver injury from tumor necrosis factor-alpha antagonists: analysis of thirty-four cases. Clin Gastroenterol Hepatol 2013;11:558–64 [e3].
[41] Borman MA, Urbanski S, Swain MG. Anti-TNF-induced autoimmune hepatitis. J Hepatol 2014;61:169–70.
[42] Liu J, Han L, Zhu L, Yu Y. Free fatty acids, not triglycerides, are associated with non-alcoholic liver injury progression in high fat diet induced obese rats. Lipids Health Dis 2016;15:27.
[43] Mantena SK, King AL, Andringa KK, Eccleston HB, Bailey SM. Mitochondrial dysfunction and oxidative stress in the pathogenesis of alcohol- and obesity-induced fatty liver diseases. Free Radic Biol Med 2008;44:1259–72.
[44] Eissing L, Scherer T, Todter K, Knippschild U, Greve JW, Buurman WA, et al. De novo lipogenesis in human fat and liver is linked to ChREBP-beta and metabolic health. Nat Commun 2013;4:1528.
[45] Kuda O, Rossmeisl M, Kopecky J. Omega-3 fatty acids and adipose tissue biology. Mol Aspects Med 2018;64:147–60.